e-ISSN: 2689-4934

Available online at
http://uppp.uitm.edu.my/online-issues.html

ESTEEM Academic Journal Vol 20, September 2024, 100-116

ESTEEM
Academic Journal
(EAJ)

Performance of thermoelectric generator system to generate electrical output from a low-grade waste heat temperature under linear and swirling waste heat streams

Muhammad Hadrami Hamdan[1], Nur Faranini Zamri[1*], Muhammad Fairuz Remeli[1], Nabilah Huda Mohd Hanim[1], Hafizah Jamilah Mohd Fatmi Shah[1], Wan Ahmad Najmi Wan Mohamed[1,2]

[1]*School of Mechanical Engineering, College of Engineering, Universiti Teknologi MARA, 40450, Shah Alam, Selangor, Malaysia*
[2]*Efficient Energy Conversion Technologies (EECT) Research Group, College of Engineering, Universiti Teknologi MARA, 40450, Shah Alam, Selangor, Malaysia*

ARTICLE INFO

Article history:
Received 30 June 2024
Revised 22 August 2024
Accepted 30 August 2024
Online first
Published 30 September 2024

Keywords:
Thermoelectric generator
Swirl flow
Fuel cell
Energy recovery
Forced convection

DOI:
10.24191/esteem.v20iSeptember.1865.g1819

ABSTRACT

A thermoelectric generator (TEG) module converts heat directly into electrical energy. Waste heat from a process is a viable heat source for TEG modules to support the energy sustainability agenda. A module was designed to recover low-temperature waste heat from a 1 kW fuel cell stack used in a mini hydrogen vehicle. The module was constructed using a single TEG cell that receives heat directly on its surface from the waste heat stream, coupled with a heat pipe connected to a finned heat sink to effectively cool the cold junction of the TEG cell. This research presents a comparison of the module characteristics when it is operated under direct impinging jet flow and swirl flow waste heat streams at 60°C, while the cold junction of the cell is cooled under stationary vehicle conditions (natural convection cooling) and cruising conditions (forced convection cooling) at an air speed of 5 m/s. Results indicate that the swirling effect increases the maximum power point (MPP) by 60%. The introduction of swirl to the heating stream is a viable approach to significantly enhance the recovery of low-grade waste heat using TEG. However, the MPP shows a greater increase of 70 to 80% due to the forced cooling effect, indicating that cold junction cooling has a more significant influence on the MPP compared to the swirl effect.

[1*] Corresponding author. *E-mail address:*nurfaraninizamri@gmail.com
https://doi.org/10.24191/esteem.v20iSeptember.1865.g1819

1. INTRODUCTION

Waste heat recovery (WHR) is an important strategy towards realising the Sustainable Development Goal 7th agenda on Efficient Energy Utilisation. WHR technologies are being continuously developed and improved to extract the excess heat energy generated from a process or system and reuse it to generate electrical and mechanical power. Approximately 20% of industrial waste heat has the potential to be reused, depending on the quality of waste heat temperature grades. High grade waste heat is categorised at temperatures greater than 400ºC, medium grade between 100ºC and 400ºC, while low grade is waste heat below 100ºC [1].

A thermoelectric generator (TEG) is a solid-state semiconductor device governed by the Seebeck effect and is viewed as a viable approach in WHR. The Seebeck effect is the capability of a semiconductor material to excite free electrons due to the flow of thermal energy [2]. In general, inducing heat transfer across a TEG cell leads to the generation of electrical power and the rate of heat transfer is influenced by the temperature difference along the cell junctions or opposite surfaces. A TEG is a viable technical solution for industrial WHR due to its benefits of long service life, no moving parts, low maintenance and zero pollution [3]. Due to the current limitation in the operating temperature of current TEG materials, which is approximately 200°C for Bismuth-Telluride [4], studies on TEG application and design modules are mostly focused on medium-grade WHR such as biomass dryers [5], automotive exhaust [6], as well as in carbonisation [7] and blast furnaces [8].

The thermoelectric effect is also observed for low-grade waste heat, making it suitable for WHR of a hydrogen fuel cell that generates waste heat in the range of 50°C to 60°C [9]. Case studies that have been reported in this area are for modelling of the energy recovery from a fuel cell stack [10], TEG module designs for mini fuel cell vehicles [11-12], single and double cell stacked configuration [13] and an advanced WHR design with hydrogen preheating for fuel cell power enhancement [3].

The power output of TEG cell is linked to design factors such as application, arrangement, and heat source. Different TEG module designs have been proposed to enhance the outputs of a module design for specific applications. An effective TEG module allows simultaneous heating and cooling of the TEG cells on its opposite surfaces to create a large temperature difference that leads to heat transfer through the semiconductor elements. Therefore, it is important for TEG module designs to have effective heat capture and dissipation mechanisms to obtain an optimised power generation. Improved modules are continuously explored due to the difference in waste heat grade, logistic constraints such as space, and practical limitations [14].

Relatively, Mohamed et al. [15] proved on a fuel cell vehicle WHR simulation that the TEG power generation is highly sensitive towards the TEG cooling rates compared to the heating rates. This is also supported by the subsequent modelling of TEG heat transfer mechanics by Mohamed et al. [16]. At a cooling air temperature of 25°C, the power output is 12% higher than at 35°C. It was proven experimentally by Makki et al. [17] that the use of heat pipes and plate-finned heat sinks enhances TEG outputs by 12.2%. The combination of TEG cells, heat pipes and heat sinks are seen as the best combination for effective heat recovery especially for low grade waste heat [12]. Thus, improving the cold junction heat transfer rates through active forced cooling is the key for high-performance TEG module designs. Recent proposals include designs that integrate heat collectors, TEG, and water-cooled heat sinks [17], as well as low thermal resistance heat exchangers [18].

This study explores the performance of a TEG module specifically designed for WHR of a fuel cell stack used in the propulsion system of a hydrogen mini vehicle. A 1 kW open-cathode Polymer Electrolyte Membrane (PEM) fuel cell generates heat at approximately 60°C at peak power. A single-cell TEG module is designed with a heat pipe and finned heat sink at the cold junction to assist in cell cooling via the motion of the vehicle. The temperature and power output profiles are experimentally analysed based on two waste

https://doi.org/10.24191/esteem.v20iSeptember.1865.g1819

heat flow configurations – direct impinging jet (Sn 0) and swirl flows (Sn 1.6). The analysis provides a scientific relationship between the effect of stream flow configuration on the cooling modes of a TEG module and is significant in advancing knowledge on enhanced TEG module designs for practical applications.

2. METHODOLOGY

2.1 TEG module design

A TEG module system is designed for a fundamental characterisation study based on a 1 kW PEM mini fuel cell vehicle (FCV). The fuel cell is the source for powering the vehicle while the stack is cooled down by surrounding air. From the highly exothermic reactions, the fuel cell produces low-temperature waste heat. Fig. 1 shows the developed TEG module which consists of a TEG cell, heat pipes and a double heat sink. The TEG cell is placed at the front of the module system to ensure both direct and swirl heat flows are facing the hot junction surface of the TEG. Thermal paste is used to attach the TEG cell to the heat sinks and eliminate air gaps for lower surface resistance. Minimal contact resistance is very important to generate optimal electrical output from TEG [19]. A thermal paste with a conductivity of 3 W/m.°C is applied between the TEG cell and the aluminum plate. Double heat sinks provide a larger surface area for heat dissipation. Heat pipes transfer heat at a very high rate for minimum heat loss through the length [16].

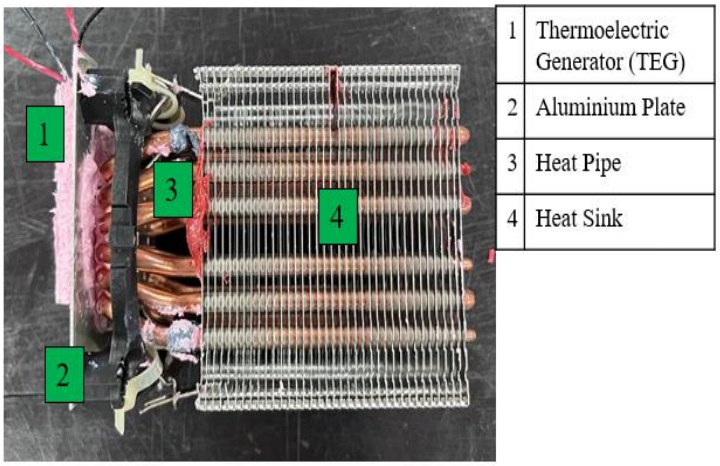

Fig. 1. TEG module design concept

2.2 Experimental setup

The system setup is designed to imitate the WHR from a mini fuel cell vehicle. The design of the test bench is based on the stack output that produces waste heat at approximately 60 °C at peak power [13]. The WHR system consists of a heating element, power-generating section, and a cooling section. **Error! Reference source not found.**2(a) shows the test bench design and setup while Fig. 2(b) is the equivalent schematic diagram. A heat gun is used as the heating element to imitate the temperature of the waste heat stream from the fuel cell stack. A thermocouple is placed near the heat gun nozzle, ensuring the hot stream temperature is approximately maintained around 60 °C with ± 1 °C tolerance. Swirl flow of the waste heat is produced by the addition of a nozzle after the heat gun. The swirl effect is generated by the fluid moving

https://doi.org/10.24191/esteem.v20iSeptember.1865.g1819

in a spiral path, rotating around a central axis. It leads to a formation of a vortex, where the fluid velocities are the highest near the center of the swirl and decrease outwards.

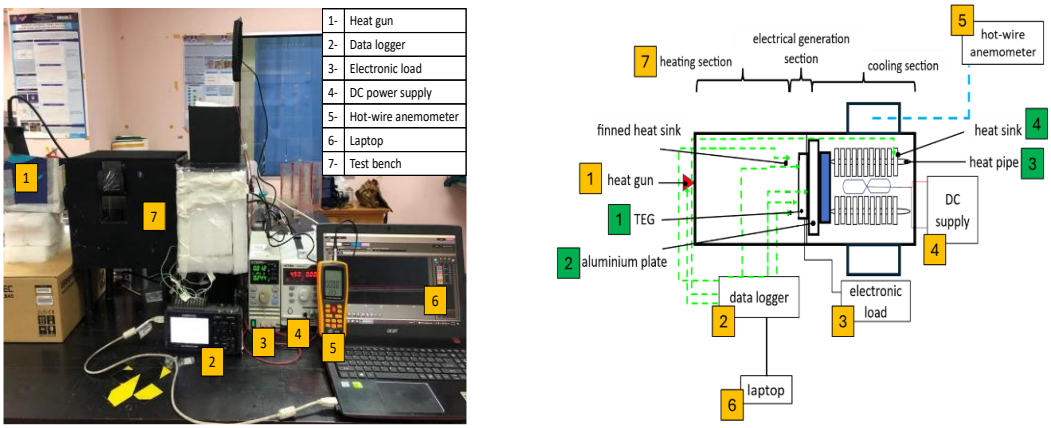

(a) (b)

Fig 2. (a) Experimental setup and, (b) Schematic diagram of the WHR system

The development of swirl increases turbulence for a more effective heat transfer. The intensity of the swirl flow is determined through the swirl number (Sn), that is defined as the ratio of the angular momentum to its axial momentum. Assuming the axial velocity of the flow is uniform, Sn is calculated by using Eq. (1).

$$S_n = \frac{{D_t}^2 + {D_h}^2}{2{D_t}^2} \tan \theta_m \quad (1)$$

where D_t is the tip diameter of the nozzle, D_h is the hub diameter of the nozzle and θ_m refers to the vane angle, as referred to Fig. 3 and Table 1.

https://doi.org/10.24191/esteem.v20iSeptember.1865.g1819

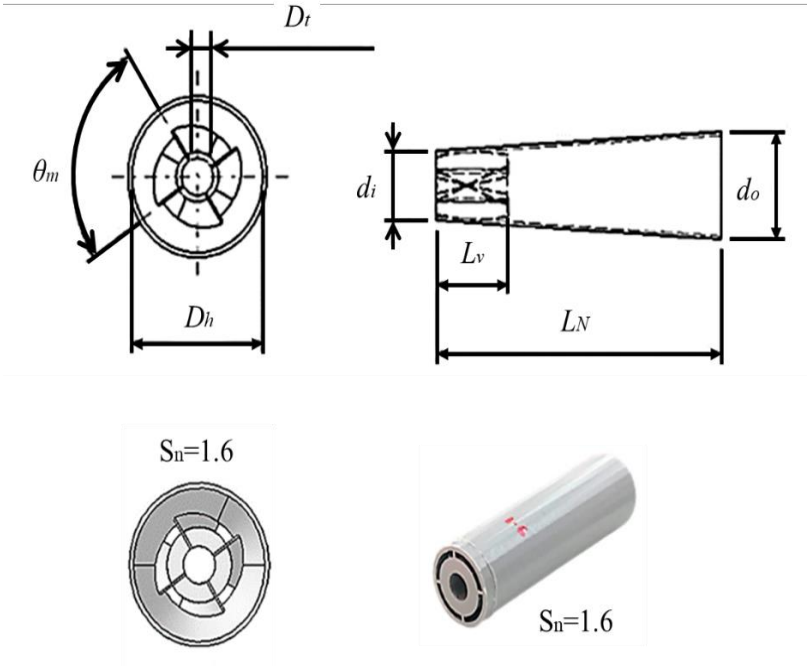

Fig. 3. The nozzle geometry and swirl designs

Table 1. Nozzle design parameters

Parameter	Symbol (unit)	Sn= 1.6
Vane angle	θ_m	65
No. of vane		4
Vane length	L_v	50
Tip diameter	D_t	40
Hub diameter	D_h	30
Inlet diameter	d_i	63
Outlet diameter	d_o	40
Nozzle length	L_N	200

The TEG hot surface is exposed directly to the waste heat stream while the cold side is attached to a double finned-type heat sink in the cooling section. As the principle of TEG requires higher temperature difference for higher electrical output, heat pipes are coupled with the heat sinks for greater heat dissipation. A higher rate of heat dissipation allows lower temperature at the cold side of the TEG surface. Table 2 provides the description of the main components used in the research work.

Table 2. Component specifications for the TEG module

Component	Descriptions
Thermoelectric generator (TEG)	Material: Bismuth Telluride
	Dimension: 60 mm x 60 mm x 4.5 mm
Heat pipe	Working fluid: Water
	Diameter: 6 mm

https://doi.org/10.24191/esteem.v20iSeptember.1865.g1819

	Length: 148 mm
Heat sink	Type: Plate-finned heat sink
	Dimension: 117 mm x 45 mm x 1 mm
	Number of fins: 55
	Gap between fins: 1 mm

The main objective of the study is to evaluate the performance of a thermoelectric generator system to generate electrical output from low-grade waste heat, under linear and swirling waste heat streams. A direct impinging jet waste heat stream is achieved by pointing the heat gun directly perpendicular to the TEG hot surface. Swirling streams results in spinning streamlines created by a swirling nozzle. Swirling flow is created as the fluid flow meets a rotational component, causing the fluid particles to follow the spiral or helical trajectory, due to the presence of angular momentum. A swirling nozzle with swirl number (Sn = 1.6) is placed at the tip of the heat gun, before directing it towards the TEG hot surface. Compared to linear fluid flow, swirling flows are expected to improve surface contact due to higher free stream velocity [19].

Equally important in the study is the effect of cooling conditions to create the optimum temperature difference of the TEG cell. The cooling of the TEG is performed at two different conditions which are natural (NC) and forced cooling (CSV 5 m/s) to imitate the FCV at rest and while moving. A DC fan is switched off for natural cooling of the TEG. In the forced cooling condition, the fan speed is set at 5 m/s (equal to 18 km/h) to simulate the motion of the FCV at a normal cruising speed. Due to the limitations of surrounding conditions, the cooling supply temperature (CST) is fixed at 22 °C. Overall, a total of four cases are tested under similar heating conditions. A summary of the parameters in the experiment is presented in Table 3. The effect of linear (Sn 0) and swirl flow Sn 1.6) are applied to the heating condition to observe the effect on the heat transfer mechanics. In the cooling section, the system performance is based on the natural cooling (NC) and forced cooling (CSV 5 m/s) for heat dissipation.

Table 4 lists the equipment and instruments installed on the test bench. The analysis in the study requires two major outputs which are by the generated electrical power from TEG and temperature profiles. TEG electrical power is measured by the electronic load, where the current and voltage are measured as the external load resistance applied to the TEG cell, which is varied between 0 Ω and 200 Ω.

Temperature measurement is essential especially at the hot and cold surface of TEG to ensure the values are consistent with the electrical power generated. Thermocouple wires are attached to ten specific points in the TEG system and connected to a data logger for real-time measurement. Data logging is also important in ensuring the system is in a steady-state condition for data analysis. A steady-state condition in a WHR system eliminates significant temperature changes in the system that instantly affect power generation.

In testing the potential of the TEG system developed, the ten specific points for temperature measurement are mapped based on the thermocouple position. The main temperature points include the heat source (waste heat temperature) and TEG hot and cold junctions ($T_{TEG,H}$, $T_{TEG,C}$). All positions are presented in relative distance (x/L), where each position is based on the overall distance between the heat source and the cooling outlet. Fig. 2 shows the positions of each temperature point where the total distance (L) is measured from the heat source (T1) to the ambient measurement point (T4) which is positioned 10 mm from the cooling heat sink. The heat source (fuel cell stack) is placed approximately 300 mm from the TEG hot surface. The study conducted mainly focuses on the TEG cell zone, referred to as T2 and T3 (relative distance x/L from 0.744 to 0.756), while the heat pipe section covers the relative distance from 0.756 to approximately 0.84.

https://doi.org/10.24191/esteem.v20iSeptember.1865.g1819

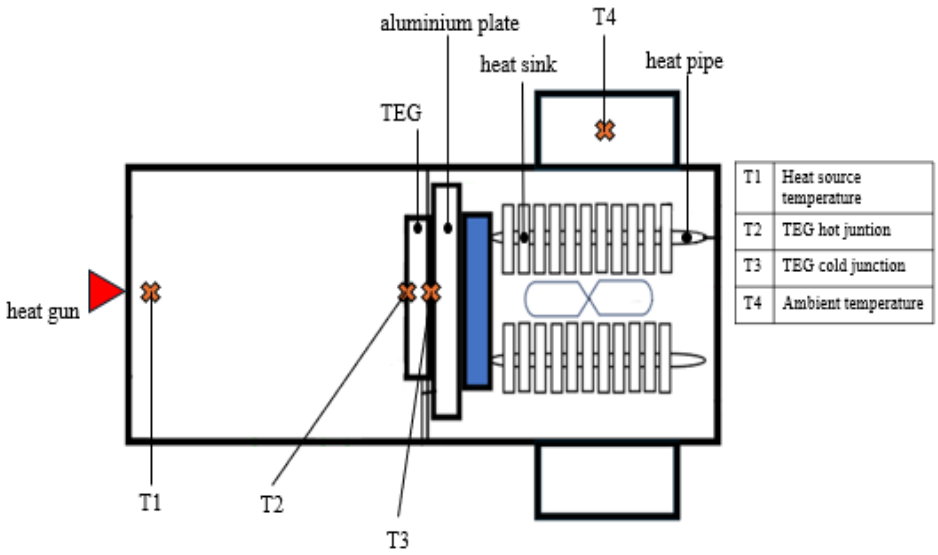

Fig. 2. Temperature points for relative distance (x/L)

Table 3. Parameters of the experiment

Parameter	Unit	Value
No. of cell	-	1
Waste heat temperature (WHT)	°C	60
Waste heat type	-	Linear (Sn 0) Swirl (Sn 1.6)
Cooling supply temperature (CST)	°C	22
Cooling condition		Natural convection (NC) Forced convection (CSV = 5 m/s)

Table 4. Specifications of the equipment and instruments for performance testing

Equipment/Instruments	Model	Descriptions
Heat gun	Steinel HG3000 SLE	Acts as heat source
Data Logger	Graphtec Midi Logger GL840	20 channels & multi-input Temperature monitoring and recording
Electronic Load	BK Precision 8540DC	Current and voltage monitoring for TEG
DC Power Supply	Atten APS3005D Regulated Power Supply	Provides direct current (DC) voltage
Hot Wire Anemometer	Benetech Hot Wire Anemometer GM8903	Measure instantaneous flow velocity and temperature
Thermocouple Wires	K-type & twin twisted	Sense temperature as connected to data logger
Thermal Paste	RS 193-8248 Silicone Thermal Putty	Eliminate air gaps from the interface area

2.3 Electrical output analysis

The electrical power output from the WHR system is obtained by increasing the external load resistance applied to the TEG. Current-voltage (IV) and power-voltage (PV) curves are the main polarisation plots. The electrical power output from the TEG is obtained through the formula in Eq. (2), where P, I and V are the TEG power output in milliwatt (mW), current in milliampere (mA) and voltage in millivolt (mV).

https://doi.org/10.24191/esteem.v20iSeptember.1865.g1819

$$P = IV \tag{2}$$

The resistance of the TEG cell is determined from Eq. (3), based on Ohm's Law, where R is the TEG resistance in Ohm (Ω).

$$V = IR \tag{3}$$

The maximum power point (MPP) is identified from the power-outage (PV) curve as the peak value. The MPP of TEG occurs when the external load resistance matches the internal resistance of the TEG cell [20].

Determination of the heat transfer coefficient is based on the rate of heat transfer across the TEG cell under steady-state conditions. As the system reaches steady-state, it is assumed that the heat transfer across the system is equivalent. TEG heat transfer rate (Q_{TEG}) is calculated based on Eq. (4), where k_{TEG}, A_{TEG}, ΔT_{TEG} and d_{TEG} are the thermal conductivity, surface area, temperature difference and thickness of the TEG cell.

$$Q_{TEG} = \frac{k_{TEG} A_{TEG} \Delta T_{TEG}}{d_{TEG}} \tag{4}$$

Under steady-state conditions, the convection heat transfer rate at the front of the TEG is assumed to be equal to the magnitude of the conduction heat transfer rate between the hot and cold surface of the cell. Thus, the coefficient of heat transfer (h) is calculated by referring to Eq. (5), where Q_{CONV}, A_{TEG}, $T_{H,IN}$ and $T_{TEG,H}$ refer to the convection heat transfer rate (W), TEG surface are (m^2), hot airstream temperature (°C) and TEG hot surface temperature (°C).

$$Q_{CONV} = hA_{TEG}\left(T_{H,IN} - T_{TEG,H}\right) \tag{5}$$

3. RESULT AND DISCUSSION

The purpose of the experiment is to obtain the combined responses of the TEG system, influenced by the heating and cooling flow conditions. The results are discussed according to this chronology:

(i) Analysis of the temperature profiles and heat transfer across the module,
(ii) Characterisation of the electrical behaviour, mainly on cell polarisation and maximum power point (MPP).

3.1 Temperature profile

The temperature profiles of each case study are presented in Fig. 3, focusing on the TEG cell zone (relative distance x/L from 0.744 to 0.756). The total distance (L) is measured from the heat source (heat gun) to the ambient measurement point which is positioned 10 mm from the cooling heat sink. The heat pipe section covers the relative distance from 0.756 to approximately 0.84.

The fuel cell stack (heat source) is located approximately 300 mm from the TEG cell. The waste heat stream suffers a significant temperature reduction by approximately 13 °C as it reaches the TEG cell hot junction due to ambient cooling. At the TEG hot surface (hot junction), the temperature is 47 °C. The

https://doi.org/10.24191/esteem.v20iSeptember.1865.g1819

temperature on the TEG hot side surface is consistent at 47ºC for both linear and swirl streams. However, the temperature profile across the TEG cell is different at similar cooling modes due to the influence of the heating stream flow configuration on the convection heat transfer mechanics of the TEG hot-side surface. It is observed that swirl flows enhance the convection heat transfer and enable greater heat flow rates through the TEG cell at similar cooling conditions which lead to higher temperature drop. The swirl effect on the waste heat stream temperature seems to be negligible in this case study due to the controlled experiment setup. However, the swirling flow has a positive effect on the convection mechanics of the TEG surface, allowing higher heat transfer rates by convection to the TEG cell surface and consequently resulting to a greater heat flow by conduction through the TEG cell under similar cooling modes. This indicates the importance of optimising the stack-to-TEG distance to obtain a greater energy potential at the TEG surface. However, the distance must consider the required space for effective back pressure to induce air (suction force) into the PEM fuel cell stack.

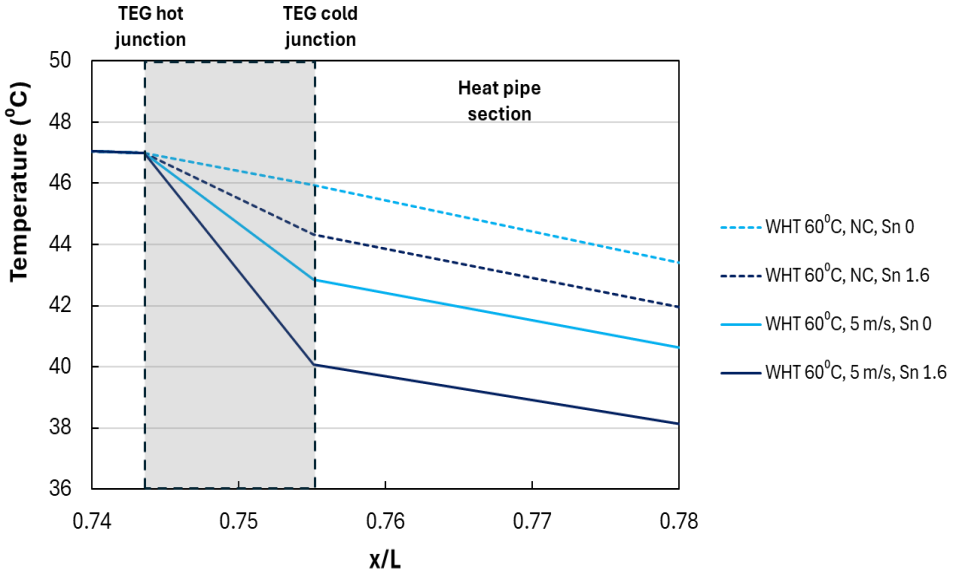

Fig. 3. Temperature profiles across the TEG cell and heat pipe under variation of hot stream flow configuration and cooling conditions

The temperature profiles for both natural convection and forced convection cooling indicate that temperature differences exist across the TEG cell mainly due to the conversion of thermal energy into electricity. The temperature gradient is larger for swirl flows compared to direct impinging jet flows, as well as in cases involving forced convection cooling at the cold side of the TEG module. This analysis underscored the sensitivity of heat transfer within the TEG cell to the effectiveness of the cooling mechanism, as proven by the TEG model developed by Mohamed et al. [16].

Fig. 4 provides the comparison of TEG temperature difference under the different cases. For the basic case of direct impinging waste heat streamlines towards the TEG surface, the cell temperature difference is only 1°C for natural convection cooling at the heat sink, while it is 2.5 ºC under forced convection cooling (5 m/s). However, the heat transfer mechanics across the TEG cell are significantly enhanced by the swirling flows. Under forced convection cooling at the heat sink, the temperature difference increases between 150% to 200% compared to natural cooling, leading to larger heat transfer rates across the TEG cell, as shown in Fig. 5. The forced convection cooling enhances the heat dissipation and lowers the

https://doi.org/10.24191/esteem.v20iSeptember.1865.g1819

temperature of the TEG cold surface for higher temperature difference across the cell. This proves that both the temperature difference and heat transfer are sensitive to active cooling.

Fig. 6 compares the heat transfer coefficient at the TEG hot surface junction with respect to different hot stream flow conditions. The heat transfer coefficient (h) is calculated based on the steady state condition during the experiment, for both direct Sn = 0 and swirl Sn = 1.6 under waste heat temperature (WHT) of 60 °C and different cooling conditions (natural and forced convection). Under a direct or linear (Sn = 0) heating stream, the value of the value of h is between 30 to 100 W/m^2.°C, under natural and forced cooling (5 m/s) condition. For Sn = 1.6, the h ranges between 80 to 140 W/m^2.°C, and it proves that swirling flow of the heating stream greatly enhances the heat transfer coefficient. The values of h for Sn = 1.6 are approximately 151% and 40% higher compared to direct impinging jet flows for natural and forced cooling. The incoming swirling hot fluid has a greater heat contact with the TEG hot surface that results in greater Nusselt numbers (Nu). It allows higher rate of convection heat transfer towards the TEG; hence, it produces higher heat transfer coefficient. These results have similar pattern with the findings of Singh et al. [19] where direct impinging jet flow offers lower thermal reactions at the TEG hot surface.

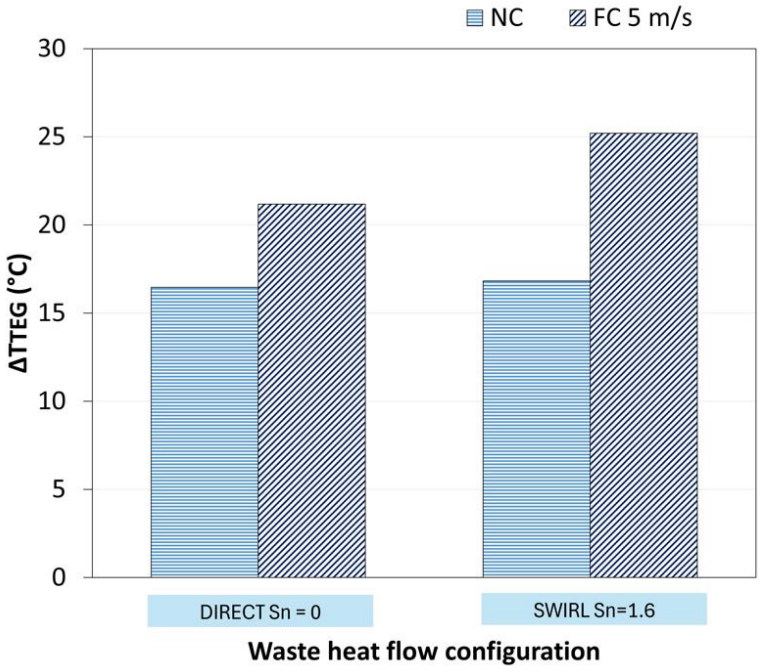

Fig. 4. Temperature difference across the TEG cell at a WHT of 60 °C

https://doi.org/10.24191/esteem.v20iSeptember.1865.g1819

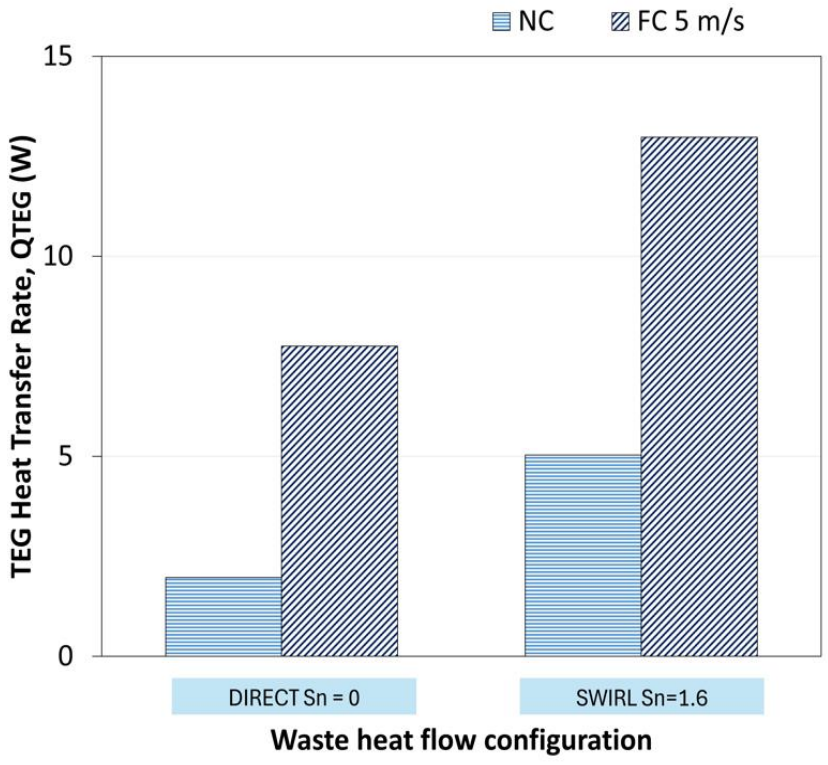

Fig. 5. Heat transfer rate across the TEG cell

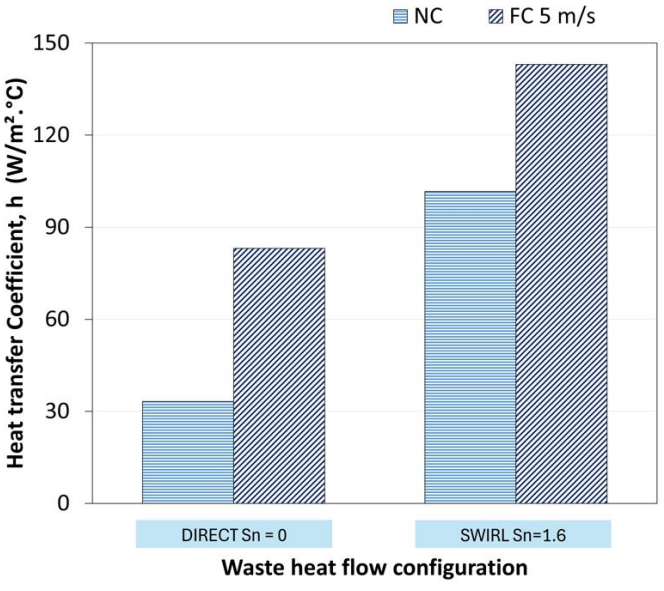

https://doi.org/10.24191/esteem.v20iSeptember.1865.g1819

Fig. 6. Convection heat transfer coefficient at the TEG hot surface junction

3.2 Electrical profile

Fig. 7 provides the profiles of the thermoelectric cell polarisation under direct hot stream flow and swirl flow. Varying the circuit resistance yields a linear I-V profile where higher currents are generated at low cell voltages. This behaviour satisfies the Ohm's Law that stated the current and voltage are inversely linear as external resistances are applied and they are similar to the I-V profiles of a TEG module design by Rashid et al. [3] and Sulaiman et al. [12]. Open circuit voltage (V_{OC}) is the voltage measured across the TEG cell when no external load is applied. Higher V_{OC} generally indicates the TEG cell potential in generating electrical output due to specific temperature differences, as well as an indicator of the efficiency of the thermoelectric material. The V_{OC} is the highest at 220 mV for the combined configuration of swirling flow at the hot junction and forced cooling of the cold junction. The configuration of direct hot stream flow with natural convection cooling only yields approximately 110 mV.

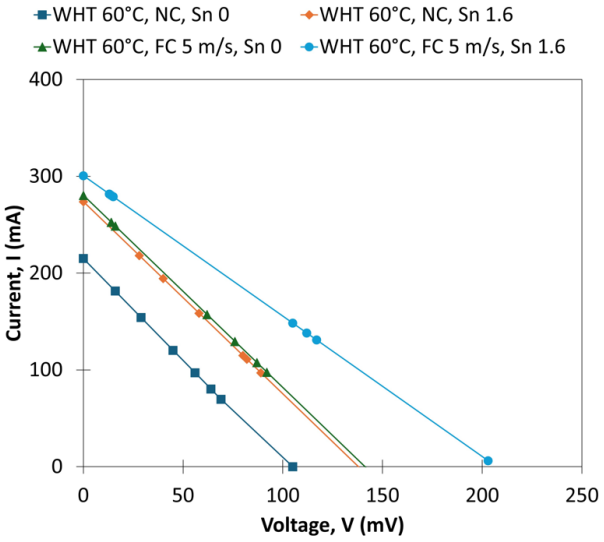

Fig. 7. I-V and polarisation profiles of the TEG module at WHT= 60 °C

The parabolic cell polarisation curves in Fig. 8 indicate that as the cell voltage gradually increases, the electrical power output increases to a maximum power output (MPP) before the generated power reduces due to the conductance capacity limit of the thermoelectric material, relative to the temperature difference between the cell junctions. A good TEG module design, assembly and operation would yield a larger polarisation curve as the voltage increases. It is evident that operating the system under swirl hot stream flow coupled with forced cooling generates higher power outputs due to higher temperature difference generated across the junctions as discussed previously. The V_{OC} for swirl flow with natural convection cooling is approximately similar to the V_{OC} of direct hot stream flow with forced convection cooling at 140 mV. The cell energy potential of the swirl hot stream flow significantly increases by 60% to 220 mV when forced cooling is applied.

https://doi.org/10.24191/esteem.v20iSeptember.1865.g1819

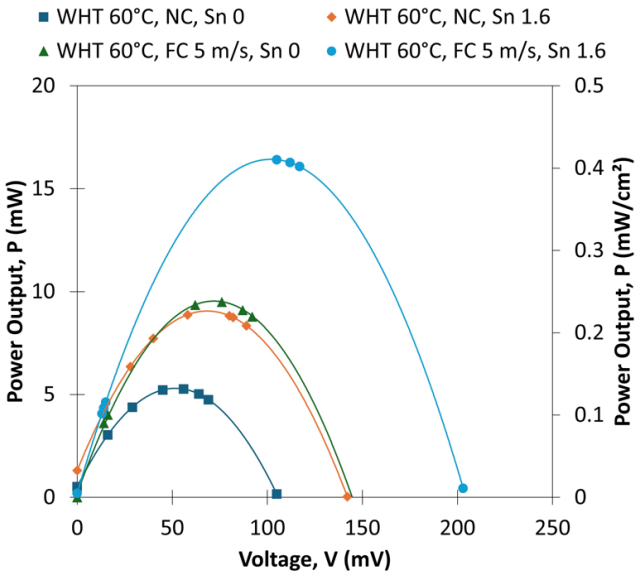

Fig. 8. P-V and polarisation profiles of the TEG module at WHT= 60 °C

Error! Reference source not found. shows the MPP comparison for all cases. The MPP for the swirling hot stream flow is generally 60% higher under similar cooling conditions. Operating the system under forced convection cooling with a nominal air velocity of 5 m/s increases the power output by a range of 70 to 80%, which is higher than the effect of swirl at the hot junction. This is supported by the results of a parametric sweep analysis and experiments of Zamri et al. [14] and Mohamed et al. [16] for a TEG assembly where the power output of a TEG system is most sensitive to the cooling conditions at the cold junction compared to other operating and geometrical parameters. Therefore, the design and operation of the TEG cold junction cooling are essential aspects in optimising the electrical outputs from a thermoelectric system.

The maximum power point (MPP) for each case occurs at a specific voltage, determined by adjusting the external resistance (R_L) applied to the TEG cell. As shown in Fig 9(a), the highest V_{MPP} of 105 mV is achieved with a swirl nozzle S_n of 1.6 and active cooling at 5 m/s. When comparing different cooling methods, the 5 m/s airflow produces a greater V_{MPP}, with the swirl nozzle further enhancing the voltage. Under the natural cooling mode (NC), the swirl nozzle with S_n of 1.6 has a negligible impact on V_{MPP}. However, in the 5 m/s cooling mode with S_n of 1.6, the voltage potential significantly improves. This behaviour is consistent with the temperature profile discussed in Section 3.1. The NC has the least temperature difference, which indicates a slower heat transfer and relates to the lowest electrical performance. As TEG is directly correlated to the thermal behaviour, the temperature increment accelerates the electron kinetic energy, which excites more charge carriers that move from the hot side to the cold side of the TEG. This movement generates an electrical potential difference, or voltage (V).

https://doi.org/10.24191/esteem.v20iSeptember.1865.g1819

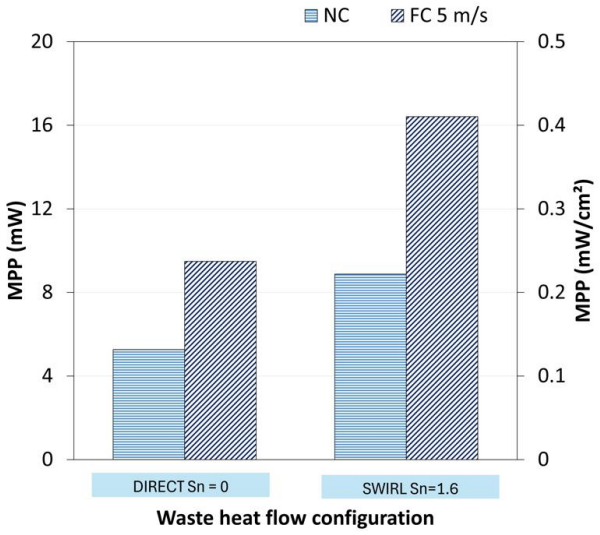

Fig. 11. Comparison of MPP for variations in the waste heat flow configuration

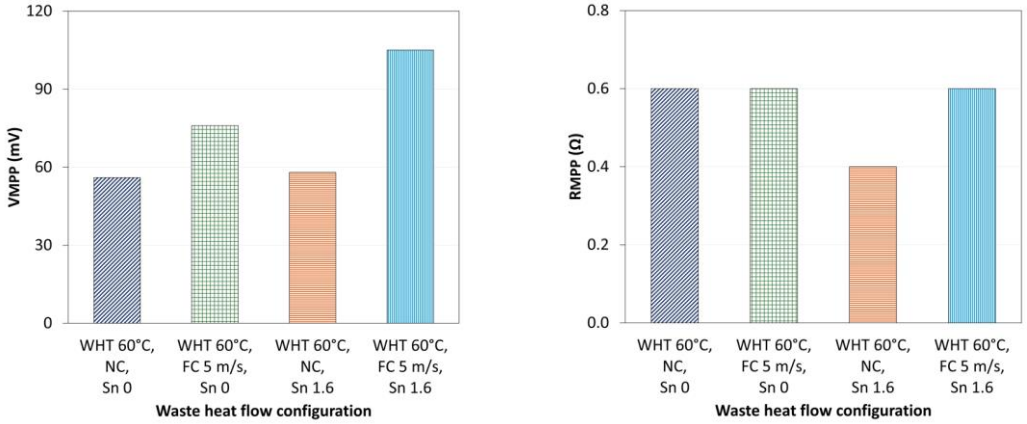

(a) (b)

https://doi.org/10.24191/esteem.v20iSeptember.1865.g1819

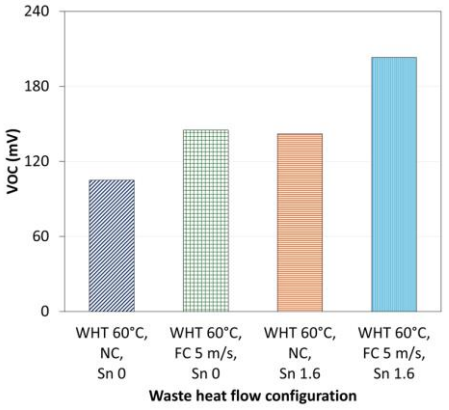

(c)

Fig 9. Profiles of (a) Cell voltage at MPP (V_{MPP}), (b) Circuit resistance at MPP (R_{MPP}), and (c) Open circuit voltage (V_{OC})

A greater temperature difference leads to more energetic charge carriers and a higher voltage potential. Therefore, a higher V_{MPP} reflects the TEG cell's enhanced ability to generate maximum power, contributing to better efficiency and improved performance monitoring and control. R_{MPP} is the resistance value at which MPP is produced from the TEG cell, as the external load applied to the TEG equals the internal resistance of the cell. From Fig 9(b), the R_{MPP} ranges between 0.4 Ω and 0.6 Ω for all four cases. The TEG cell has demonstrated the ability to produce the MPP at a constant and low range of external load. As shown in Fig 9(c), the V_{OC} ranges between 100 to 200 mV which corresponds to the TEG's highest electrical output and temperature difference. V_{OC} improves as a result of a greater temperature gradient across the TEG, which increases the Seebeck voltage generated. This is because a larger temperature difference enhances the thermoelectric effect, driving more charge carriers and resulting in higher voltage potential.

4. CONCLUSION AND RECOMMENDATION

The manuscript presents the evaluation of the TEG system performance under both direct and swirl flow waste heat streams while comparing the effect of natural and forced cooling conditions. The TEG system has a high potential in generating electrical power even when low temperature waste heat at 60°C is directed to the module. The highest MPP of 0.4 mW/cm^2 is generated at S_n = 1.6 while forced convection cooling at 5 m/s is applied for heat dissipation. This is a significant improvement produced by the TEG system compared to a direct waste heat stream flow that only generated an MPP of 0.2 mW/cm^2. The performance analysis also detailed the fundamental heat transfer coefficients for both direct and swirl waste heat streams. The coefficient improves as the swirl flow increases the thermal contact between the fluid and the TEG hot surface. The highest coefficient produced is 143 W/m^2.°C, which also generates the highest MPP. This aligns with the heat transfer rate across the TEG cell and the temperature difference between the TEG surfaces. The active cooling applied to the heat sinks is an advantageous integration into the WHR system due to the increase in heat transfer efficiency across the TEG cell. Hence, the combination of swirl flow waste heat stream and active cooling in the WHR design is recommended for higher overall efficiency.

5. ACKNOWLEDGEMENTS

The authors wish to acknowledge the contributions of the College of Engineering, Universiti Teknologi MARA for the facilities used in this work.

https://doi.org/10.24191/esteem.v20iSeptember.1865.g1819

6. CONFLICT OF INTEREST STATEMENT

All the authors declared that this research was conducted in an unbiased manner, in the absence of any self-benefits and without financial conflicts that could lead to conflict-of-interest issues.

7. AUTHORS' CONTRIBUTIONS

Muhammad Hadrami Hamdan: Methodology, investigation; **Nur Faranini Zamri**: Methodology, formal analysis, writing-review; **Muhammad Fairuz Remeli**: Conceptualisation, supervision; **Nabilah Huda Mohd Hanim**: Methodology, investigation; **Hafizah Jamilah Mohd Fatmi Shah**: Methodology, investigation; **Wan Ahmad Najmi Wan Mohamed**: Conceptualisation, formal analysis, supervision.

8. REFERENCES

[1] M. S. Sulaiman, W. A. N. W. Mohamed, B. Singh, and M. F. Ghazali, "Validation of a Waste Heat Recovery Model for a 1kW PEM Fuel Cell using Thermoelectric Generator," in *IOP Conference Series: Materials Science and Engineering*, Institute of Physics Publishing, Aug. 2017. Available: doi: 10.1088/1757-899X/226/1/012148.

[2] S. M. Pourkiaei *et al.*, "Thermoelectric cooler and thermoelectric generator devices: A review of present and potential applications, modeling and materials," *Energy*, vol. 186, 2019. Available: doi: 10.1016/j.energy.2019.07.179.

[3] A. A. Rashid, N. Aqilah, M. Som, G. J. Jimmy, and M. H. Hamdan, "Performance Analysis on Series and Parallel Circuit Configurations of a Four-Cell Thermoelectric Generator Module Design", *Journal of Applied Engineering Design and Simulation*, vol. 1, no. 1, pp. 32-42, 2021. Available: doi:10.24191/jaeds.v1i1.18.

[4] S. H. Park *et al.*, "Fe-Ni-Cr diffusion barrier for high-temperature operation of Bi2Te3," *J Alloys Compd*, vol. 932, p. 167537, 2023. Available in: doi: 10.1016/j.jallcom.2022.167537.

[5] S. Maneewan and S. Chindaruksa, "Thermoelectric power generation system using waste heat from biomass drying," *J Electron Mater*, vol. 38, no. 7, pp. 974–980, 2009. Available: doi: 10.1007/s11664-009-0820-5.

[6] B. Orr, B. Singh, L. Tan, and A. Akbarzadeh, "Electricity generation from an exhaust heat recovery system utilising thermoelectric cells and heat pipes," *Appl Therm Eng*, vol. 73, no. 1, pp. 588–597, 2014. Available: doi: 10.1016/j.applthermaleng.2014.07.056.

[7] H. Kaibe, T. Kajihara, and S. Fujimoto, "Recovery of Plant Waste Heat by a Thermoelectric Generating System," *Komatsu Technical Report*, vol. 57, no. 164, pp. 26–30, 2011, [Online]. Available: http://dcnwis78.komatsu.co.jp/CompanyInfo/profile/report/pdf/164-E-05.pdf

[8] F. Meng, L. Chen, F. Sun, and B. Yang, "Thermoelectric power generation driven by blast furnace slag flushing water," *Energy*, vol. 66, pp. 965–972, Mar. 2014, doi: 10.1016/j.energy.2014.02.018.

[9] W. Mohamed and M. Kamil, "Hydrogen preheating through waste heat recovery of an open-cathode PEM fuel cell leading to power output improvement," *Energy Convers Manag*, vol. 124, pp. 543–555, 2016. Available: doi: 10.1016/j.enconman.2016.07.046.

[10] M. Alam, K. Kumar, and V. Dutta, "Dynamic modeling and experimental analysis of waste heat recovery from the proton exchange membrane fuel cell using thermoelectric generator," *Thermal Science and Engineering Progress*, vol. 19, no. June, p. 100627, 2020. Available: doi: 10.1016/j.tsep.2020.100627.

[11] W. Mohamed, M. H. Hamdan, N. F. Zamri, I. A. Zakaria, and M. F. Mohamad, "Integrated Heat Regenerator (IHR) Designs with Hydrogen Preheater and Thermoelectric Generator for Power Enhancement of a 2 kW Fuel Cell Vehicle," *International Journal of Integrated Engineering*, vol. 0, pp. 1–4, 2021.

https://doi.org/10.24191/esteem.v20iSeptember.1865.g1819

[12] M. Saufi Sulaiman, B. Singh, and W. A. N. W. Mohamed, "Experimental and theoretical study of thermoelectric generator waste heat recovery model for an ultra-low temperature PEM fuel cell powered vehicle," *Energy*, vol. 179, pp. 628–646, 2019. Available: doi: 10.1016/j.energy.2019.05.022.

[13] W. A. N. W. Mohamed, N. F. Zamri, M. H. Hamdan, H. J. M. F. Shah, and N. H. M. Hanim, "Performance of Single Cell and Double Stacked Thermoelectric Generator Modules for Low Temperature Waste Heat Recovery," *IOP Conf Ser Earth Environ Sci*, vol. 1261, no. 1, 2023. Available: doi: 10.1088/1755-1315/1261/1/012007.

[14] N. F. Zamri, M. H. Hamdan, S. N. A. Anuar, W. A. N. W. Mohamed, and M. F. Remeli, "Performance of A Plate-Finned Thermoelectric Generator (TEG) Module for Industrial Waste Heat Recovery," *Journal of Mechanical Engineering*, vol. 19, no. 3, pp. 257–272, 2022. Available: doi: 10.24191/jmeche.v19i3.19817.

[15] W. A. N. W. Mohamed, B. Singh, M. F. Mohamed, A. M. Aizuwan, and A. B. M. Zubair, "Effects of fuel cell vehicle waste heat temperatures and cruising speeds on the outputs of a thermoelectric generator energy recovery module," *Int J Hydrogen Energy*, vol. 46, no. 50, pp. 25634–25649, 2021. Available: doi: 10.1016/j.ijhydene.2021.05.084.

[16] W. A. N. W. Mohamed, N. F. Zamri, and M. F. Remeli, "Principal parameters of thermoelectric generator module design for effective industrial waste heat recovery," *Journal of Thermal Engineering*, vol. 10, no. 2, pp. 457–478, 2024. Available: doi: 10.18186/thermal.1456700.

[17] A. Makki, S. Omer, Y. Su, and H. Sabir, "Numerical investigation of heat pipe-based photovoltaic-thermoelectric generator (HP-PV/TEG) hybrid system," *Energy Convers Manag*, vol. 112, pp. 274–287, 2016. Available: doi: 10.1016/j.enconman.2015.12.069.

[18] J. Chen, W. Xie, M. Dai, G. Shen, G. Li, and Y. Tang, "Experiments on Waste Heat Thermoelectric Generation for Passenger Vehicles," *Micromachines (Basel)*, vol. 13, no. 1, pp. 1–14, 2022. Available: doi: 10.3390/mi13010107.

[19] B. Singh, W. A. N. W. Mohamed, M. N. F. Hamani, and K. Z. N. A. Sofiya, "Enhancement of low grade waste heat recovery from a fuel cell using a thermoelectric generator module with swirl flows," *Energy*, vol. 236, 2021. Available: doi: 10.1016/j.energy.2021.121521.

[20] S. J. G. Cooper, G. P. Hammond, and J. B. Norman, "Potential for use of heat rejected from industry in district heating networks, Gb perspective," *Journal of the Energy Institute*, vol. 89, no. 1, pp. 57–69, 2016. Available: doi: 10.1016/j.joei.2015.01.010.

https://doi.org/10.24191/esteem.v20iSeptember.1865.g1819